THE JOURNAL OF PHYSICAL CHEMISTRY C

Article

Cite This: J. Phys. Chem. C 2019, 123, 979−984

pubs.acs.org/JPCC

# Long-Lived Dark Exciton Emission in Mn-Doped $CsPbCl_3$ Perovskite Nanocrystals

Kunyuan Xu, Jara F. Vliem, and Andries Meijerink*

Condensed Matter and Interfaces, Debye Institute for Nanomaterials Science, Utrecht University, 3508 TA Utrecht, The Netherlands

Supporting Information

**ABSTRACT:** The unusual temperature dependence of exciton emission decay in $CsPbX_3$ perovskite nanocrystals (NCs) attracts considerable attention. Upon cooling, extremely short (sub-ns) lifetimes were observed and were explained by an inverted bright−dark state splitting. Here, we report temperature-dependent exciton lifetimes for $CsPbCl_3$ NCs doped with 0−41% $Mn^{2+}$. The exciton emission lifetime increases upon cooling from 300 to 75 K. Upon further cooling, a strong and fast sub-ns decay component develops. However, the decay is strongly biexponential and also a weak, slow decay component is observed with a ∼40−50 ns lifetime below 20 K. The slow component has a ∼5−10 times stronger relative intensity in Mn-doped NCs compared to that in undoped $CsPbCl_3$ NCs. The temperature dependence of the slow component resembles that of CdSe and PbSe quantum dots with an activation energy of ∼19 meV for the dark−bright state splitting. Based on our observations, we propose an alternative explanation for the short, sub-ns exciton decay time in $CsPbX_3$ NCs. Slow bright−dark state relaxation at cryogenic temperatures gives rise to almost exclusively bright state emission. Incorporation of $Mn^{2+}$ or high magnetic fields enhances the bright−dark state relaxation and allows for the observation of the long-lived dark state emission at cryogenic temperatures.

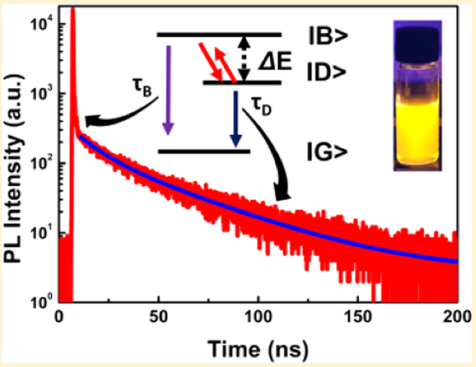


## INTRODUCTION

The discovery of $CsPbX_3$ (X = Cl, Br, I) nanocrystals (NCs) with unique optical properties has initiated a worldwide increase in research aimed at providing fundamental understanding of their peculiar properties and realizing applications of these NCs, e.g., in lighting and solar cells.[1−4] The optical properties of the $CsPbX_3$ NCs resemble those of Cd- and Pb-chalcogenide quantum dots (QDs). Bulk $CsPbX_3$ is a semiconductor. For NCs that are typically ∼10−15 nm, the exciton is confined. The NC size is however larger than the exciton Bohr radius (varying from 5 nm in $CsPbCl_3$ to 12 nm in $CsPbI_3$), giving rise to weak confinement and only small shifts of the exciton emission wavelength.[5] Tuning of the emission color is therefore not realized by size variation but by changing the chemical composition. The emission color of $CsPbX_3$ NCs can span the full visible region through anion exchange. Replacement of $Cl^-$ by $Br^-$ shifts the emission from violet to green, and subsequent replacement by $I^-$ shifts the emission further to the deep red spectral region. Additional color tuning can be realized by doping with luminescent ions (typically 3d transition metals and 4f rare earth ions) and energy transfer of the exciton to the luminescent dopant.[6−9] For applications of the perovskite NCs in light-emitting devices, not only the high quantum yield (>90%) and color tunability but also the short emission lifetime are advantageous, which is typically in the ns range at room temperature. The faster emission decay of the perovskite NCs in comparison to that of, e.g., CdSe and InP QDs has advantages in high-brightness applications. The limited stability of the perovskite NCs is a point of concern that is addressed by passivation strategies but at present hampers their application.[10,11]

In recent papers, the temperature dependence of the exciton emission lifetime was investigated for $CsPbX_3$ NCs. Both for ensemble and individual NCs, an unexpected temperature dependence was observed: upon cooling to cryogenic temperatures, the already short decay time decreased even further to sub-ns lifetimes.[12,13] This behavior is markedly different from that of the traditional Cd- and Pb-chalcogenide QDs. Typically, upon cooling, the exciton lifetime lengthens because of the energy level structure of the emitting exciton states, where the lowest energy state is a dark state that has a forbidden transition to the exciton ground state.[14−16] In well-passivated QDs, the emission from the dark state is still efficient (so the state is not really dark) but the forbidden nature causes the emission lifetime to lengthen when the system is frozen into this lowest excitonic state. For $CsPbX_3$ perovskite NCs, the opposite behavior was observed and was explained by inversion of the dark−bright state splitting induced by the Rashba effect.[12] As a result, fast bright state emission is observed at 5 K. Theoretical calculations were able

Received: December 14, 2018
Revised: December 20, 2018
Published: December 26, 2018






DOI: 10.1021/acs.jpcc.8b12035
J. Phys. Chem. C 2019, 123, 979−984

Table 1. Precursor Composition for the Synthesis of $CsPbCl_3$:$Mn^{2+}$ NCs with Various Mn-Doping Concentrations and Mn Concentrations Incorporated in $CsPbCl_3$ NCs

| Mn/Pb molar ratio | 0 | 0.5 | 1 | 2 | 3 | 4 | 5 |
|---|---|---|---|---|---|---|---|
| $MnCl_2{\cdot}4H_2O$ (g) | 0 | 0.037 | 0.055 | 0.07 | 0.079 | 0.085 | 0.089 |
| $PbCl_2$ (g) | 0.15 | 0.10 | 0.078 | 0.05 | 0.037 | 0.03 | 0.025 |
| Mn concentration in sample (atom %) | 0 | 1 | 3 | 9 | 20 | 32 | 41 |

to explain the short sub-ns lifetime. However, alternative observations were also reported. Luminescence decay measurements for $CsPbBr_3$, $FAPbBr_3$, and $FAPbI_3$, also in high magnetic fields, revealed a composition-dependent dark–bright state splitting with a lowest exciton dark state, and for $CsPbBr_3$, dark exciton emission in high magnetic fields was reported.[17−19]

Here, we report temperature-dependent luminescence lifetime measurements for exciton emission in Mn-doped $CsPbCl_3$ NCs. For different Mn-doping concentrations, we observe a clear lengthening of the exciton decay time upon cooling. Below 200 K, a rise time is observed for the exciton emission, which indicates that relaxation rates from higher exciton levels to the emitting levels slow down upon cooling. Upon further cooling, below 50 K, a biexponential decay is observed with a strong fast component (<1 ns) and a slow component develops that becomes longer-lived upon lowering the temperature. The temperature dependence of this slow component shows the typical behavior expected for a dark–bright state splitting with a lower-energy dark state. As an alternative to an inverted dark–bright splitting model, we propose that inhibited relaxation from the bright to the dark state explains the observation of fast bright state emission in $CsPbX_3$ NCs at cryogenic temperatures.

## METHODS

**Synthesis.** All of the chemicals used were obtained from Sigma-Aldrich. These include cesium carbonate ($Cs_2CO_3$), lead chloride ($PbCl_2$), manganese chloride ($MnCl_2{\cdot}4H_2O$), octadecene (ODE), oleic acid (OA), oleylamine (OM), and hexane (anhydrous). For the preparation of the cesium precursor, 0.2 g of $Cs_2CO_3$ was mixed with 7.5 mL of ODE and 0.625 mL of OA and loaded into a 50 mL flask; then, the reaction mixture was degassed, dried under 120 °C for 30 min under vacuum, and then heated at 150 °C under a $N_2$ atmosphere for additional 30 min to complete the reaction between $Cs_2CO_3$ and OA. The resulting solution was kept at 150 °C for further use. Undoped $CsPbCl_3$ NCs and $CsPbCl_3$:$Mn^{2+}$ NCs with different dopant concentrations were synthesized at a temperature of 190 °C with various Mn/Pb feeding ratios (see Table 1).

For a typical synthesis, 0.1 g of $PbCl_2$ and 0.037 g of $MnCl_2{\cdot}4H_2O$ were loaded into a 50 mL three-neck flask with 10 mL of ODE. The flask was then transferred to a Schlenk line and dried under vacuum at 120 °C for 1 h. Dried OA (1 mL) and 1 mL of OM were subsequently injected and then heated to 190 °C under a $N_2$ atmosphere. After reaching 190 °C, 0.9 mL of the hot Cs precursor was injected swiftly. The reaction was quenched 5 s later by immersion of the reaction container in an ice–water bath. The product was separated by centrifugation, washed once with acetone/hexane, and finally dissolved in 5 mL of hexane.

**Characterization.** Transmission electron microscopy (TEM) images were obtained with FEI Tecnai T20, operating at 200 kV. The samples for TEM imaging were prepared by dipping a carbon-coated copper mesh TEM grid into a hexane solution of NCs. The excess liquid was evaporated under vacuum. Luminescence (emission and excitation) spectra and photoluminescence (PL) decay curves were measured using an Edinburgh Instruments FLS920 spectrofluorometer equipped with a 450 W xenon lamp as an excitation source and a 0.22 m double grating monochromator for excitation (Bentham DTMS300, 1200 lines/mm grating, blazed at 300 nm for excitation). Emission spectra (380–700 nm) were recorded with a single 0.22 m monochromator (500 nm blazed grating), and the emitted light was detected by a Hamamatsu R928 photomultiplier tube (PMT). The fast decay profiles of the exciton emission were recorded using an Edinburgh EPL375 pulsed diode laser ($\lambda_{ex}$ = 376.8 nm and pulse width: 65 ps) with a fast Hamamatsu H74422-40 PMT to detect the emission. An Oxford Instruments liquid helium flow cryostat was used to measure the PL properties at low temperatures (down to 4.2 K). The samples for room temperature optical analysis were prepared by dissolving the crude NCs mixture in hexane and transferring the solution to a quartz cuvette. For low-temperature measurements, the NC solution was loaded in a sealed quartz cuvette.

## RESULTS AND DISCUSSION

The synthesis of the Mn-doped and undoped $CsPbCl_3$ NCs yielded cubic NCs of ∼12 nm, as shown in the TEM images in Figure 1. The actual amount of Mn incorporated in the $CsPbCl_3$ NCs was determined with energy-dispersive X-ray spectroscopy (EDX, see Table 1) and was always much lower than the amount of Mn present in the reaction mixture. After thorough washing with hexane, the Mn concentration in the NCs was determined using EDX. The samples investigated contained 0, 1, 3, 9, 20, 32, and 41% of $Mn^{2+}$. The NCs show bright luminescence with a sharp excitonic emission line at around 400 nm and a broad $Mn^{2+}$ emission band at around 600 nm. The emission spectra in Figure 1 show that the relative intensity of the $Mn^{2+}$ emission band increases and shifts to longer wavelengths for higher $Mn^{2+}$ concentrations. Upon cooling, the relative intensity of the $Mn^{2+}$ emission strongly decreases from 300 to 150 K. Below 75 K, the relative Mn-emission intensity increases again, but it remains much lower than that at 300 K (Supporting Information, Figures S1 and S2). This temperature behavior is consistent with reports in the literature and reflects the temperature dependence of the exciton-to-$Mn^{2+}$ energy transfer rate relative to processes giving rise to exciton emission.[20,21]

Luminescence decay curves were recorded for both the exciton and $Mn^{2+}$ emission between 4.2 and 300 K for $CsPbCl_3$ NCs doped with 0, 1, 3, 9, 20, 32, and 41% of $Mn^{2+}$. Here, we focus on the exciton emission decay. As an example, Figure 2 displays the luminescence decay curves for the 20% Mn-doped $CsPbCl_3$ NCs. Three temperature regimes are depicted. Between 293 and 200 K (Figure 2a), the decay curves are close to single exponential. Upon cooling from 293 to 200 K, the luminescence decay time lengthens from 0.1 ns at


DOI: 10.1021/acs.jpcc.8b12035
J. Phys. Chem. C 2019, 123, 979−984

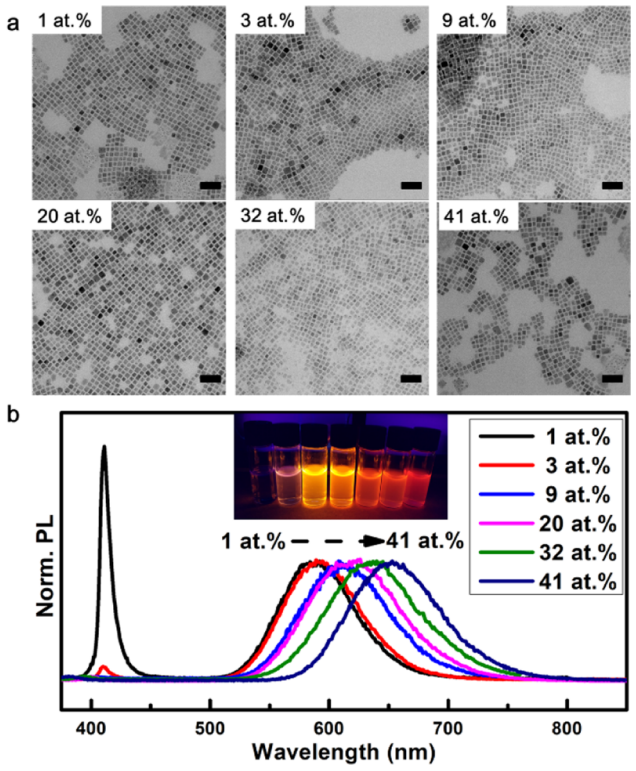


**Figure 1.** Morphology and optical properties of $CsPbCl_3$:$Mn^{2+}$ (1−41 atom %) NCs. (a) TEM images of $CsPbCl_3$:$Mn^{2+}$ NCs with different $Mn^{2+}$ concentrations (1−41 atom %, scale bar: 50 nm). (b) Emission spectra of $CsPbCl_3$:$Mn^{2+}$ NCs with different $Mn^{2+}$ concentrations (1−41 atom %, $\lambda_{ex}$ = 355 nm, inset: sample under 365 nm excitation provided by a handheld UV lamp).

293 K to 0.4 ns at 200 K and the intensity increases. This can be explained by less-efficient exciton to $Mn^{2+}$ energy transfer and is consistent with the strong decrease in the relative $Mn^{2+}$ emission intensity between 293 and 200 K. Upon further cooling to 75 K, the lengthening of the decay time continues (note the change in time scales from Figure 2a−c). In addition, the decay curves show a clear rise with a rise time that increases from 1.8 ns at 150 K to 3.2 ns at 75 K. The observation of a rise indicates that relaxation from the higher excited states (initially populated under pulsed excitation at 376 nm) to the emitting exciton states at around 400 nm slows down at cryogenic temperatures. Usually, fast (10−100 ps) relaxation is observed for relaxation to band edge states in semiconductors, but in the $CsPbCl_3$ NCs, phonon relaxation is relatively slow and the phonon population relaxation rates decrease to the ns regime upon freezing.

Upon further cooling from 75 to 4 K, the luminescence decay curves become strongly biexponential with a fast sub-nanosecond component and a slow component that lengthens as the temperature decreases from 75 to 4 K. The relative contribution of the fast component increases at lower temperatures, and the decay of the slow component slows down and stabilizes below ∼20 K. A similar behavior is observed for other high Mn concentrations. As an example Figure 2d,e shows the luminescence decay curves for the exciton emission in $CsPbCl_3$:$Mn^{2+}$ with 9 and 32 atom % $Mn^{2+}$. An overview of the temperature-dependent decay behavior of all $CsPbCl_3$:$Mn^{2+}$ (1−41 atom %) samples is given in the Supporting Information (Figures S3−S6). These results show that for low doping concentrations (1 or 3% $Mn^{2+}$) the influence of the Mn doping is not as pronounced as for $Mn^{2+}$ concentrations of 9% and higher. For all higher (9−41%) $Mn^{2+}$ concentrations, the relative intensity of the long-lived component is about 5−10 times stronger than that for undoped $CsPbCl_3$.

The present observations resemble those for the exciton emission in $CsPbBr_3$ in a magnetic field where also a fast initial decay component at low temperatures was followed by a weak and slow decay component.[19] The fast decay component was assigned to bright state exciton emission and the slow component to dark exciton emission. Slow relaxation from the bright to the dark state exciton at low temperatures can explain the observation of short-lived bright state emission decay prior to relaxation to the dark state. From the temperature dependence of the dark state emission decay time, a dark−bright state splitting of ∼8 meV was calculated for $CsPbBr_3$. Also, for CdSe QDs, an initial fast decay related to the bright state emission prior to relaxation to the dark state has been reported at temperatures below 10 K.[15] The temperature-dependent decay behavior of the exciton emission for $CsPbX_3$ NCs in a magnetic field and the present observations for Mn-doped $CsPbCl_3$ NCs can be explained by a slow bright−dark state relaxation at cryogenic temperatures. The situation is similar to that for Cd- and Pb-chalcogenide QDs but with a significant slower relaxation between excitonic states, which gives rise to the observation of the intense and fast (sub-ns) bright state emission, which dominates at cryogenic temperatures.

To test the presence of dark state emission in pure $CsPbCl_3$ NCs, we also measured luminescence decay curves as a function of temperature for undoped NCs. The temperature-dependent behavior is similar to that observed for the Mn-doped NCs, but the relative intensity of the dark state emission is much lower. As an example, Figure 3 shows the 35 K decay curves for the exciton emission in $CsPbCl_3$ NCs and $CsPbCl_3$:$Mn^{2+}$ (20 atom %) NCs. For both systems, a fast and strong initial sub-ns decay is followed by a slow temperature-dependent decay component. The amplitude for the slow component is more than 3 orders of magnitude smaller than that for the fast component. For $CsPbCl_3$ doped with 20% $Mn^{2+}$, the decay behavior is similar but the amplitude of the slow dark state emission component is about 2 orders of magnitude lower. This can be explained by a faster bright−dark state relaxation induced by the $Mn^{2+}$ dopants. Similar observations can be found in refs 18 and 19 where an increase in the relative intensity is observed for the slow decay component of the exciton emission from $CsPbBr_3$ NCs upon increasing the external magnetic field to 10[19] or 30 T.[18] Incorporation of magnetic $Mn^{2+}$ can generate a magnetic field, which has a similar effect to that of an externally applied magnetic field. This indicates that the presence of magnetic ions ($Mn^{2+}$) or an external magnetic field induces faster relaxation between the dark and bright states. The role of the magnetic field in the enhanced spin-relaxation between states with different magnetic moments may be mixing of spin states, which can also explain the shorter decay times observed for dark exciton emission in magnetic fields or upon $Mn^{2+}$ doping.[19,22] In single (undoped) dot experiments, the low count rate and more than 3 orders of magnitude higher amplitude of the bright state emission prevents the observation of the slow dark state emission. Indeed, inspection of the single $CsPbX_3$ NC exciton decay curves in ref 12 shows that the noise level starts above $10^{-3}$ in the decay curves with a maximum


DOI: 10.1021/acs.jpcc.8b12035
J. Phys. Chem. C 2019, 123, 979−984

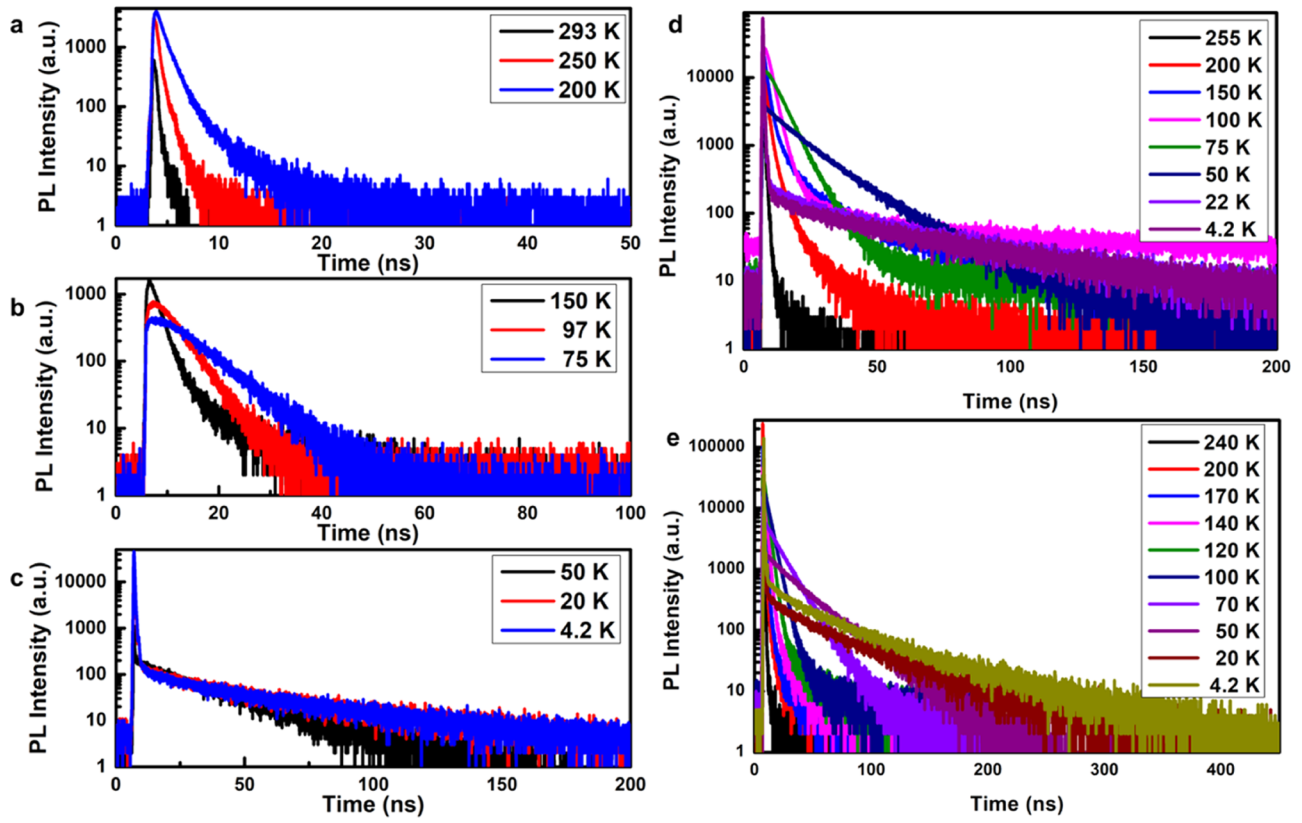


**Figure 2.** Decay curves of $CsPbCl_3:Mn^{2+}$ (20 atom %) NCs (a–c), $CsPbCl_3:Mn^{2+}$ (9 atom %) NCs (d), and $CsPbCl_3:Mn^{2+}$ (32 atom %) NCs (e) at different temperatures plotted on a semilogarithmic scale ($\lambda_{ex}$ = 376.8 nm, pulse width: 65 ps).

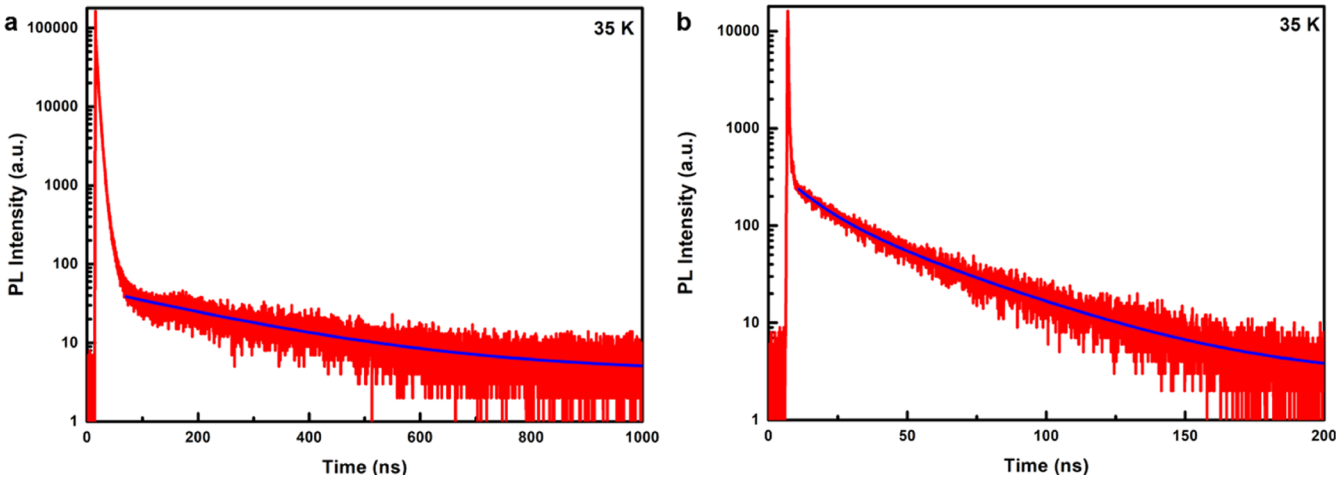


**Figure 3.** Exciton emission decay curves of undoped $CsPbCl_3$ NCs (a) and $CsPbCl_3:Mn^{2+}$ (20 atom %) NCs (b) at 35 K plotted on a semilogarithmic scale ($\lambda_{ex}$ = 376.8 nm, pulse width: 65 ps).

scaled to $10^0$, thus making it impossible to observe the slow decay component of the exciton emission.

To estimate the dark–bright state splitting, the temperature dependence of the slow decay component was analyzed for $CsPbCl_3$ NCs with 9, 20, and 32% of $Mn^{2+}$. The nearly single exponential decay in the long-time regime was fitted to exponential decay (see the Supporting Information for details, Figures S7–S9). The choice of the time interval for the fitting is somewhat arbitrary and introduces an uncertainty in the decay times. The time interval chosen is evident from the drawn lines in Figure 3 (and also in Figures S7–S9), which represent a time interval where the slow decay is close to single exponential. In Figure 4, the temperature dependence of the decay times is depicted. For all three samples, a similar behavior is observed. The decay time is constant at around 40–50 ns between 4 and 20 K and decreases strongly between 20 and 75 K. A fit of the temperature dependence to a three-level model

$$\frac{1}{\tau_{Obs}} = \frac{1}{\tau_D}\left(\frac{e^{\Delta E/kT}}{1 + e^{\Delta E/kT}}\right) + \frac{1}{\tau_B}\left(\frac{1}{1 + e^{\Delta E/kT}}\right)$$

where $\tau_{Obs}$ is the measured decay time, $\tau_D$ is the decay time of the dark state, and $\tau_B$ is the decay time of the bright state, gives



DOI: 10.1021/acs.jpcc.8b12035
J. Phys. Chem. C 2019, 123, 979–984

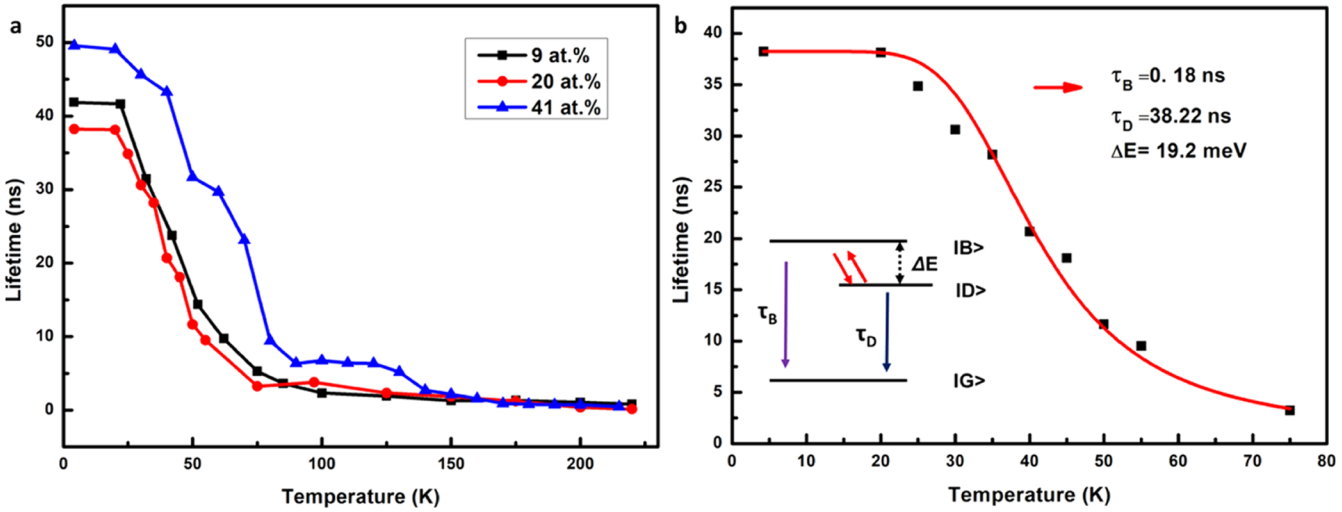


**Figure 4.** Exciton emission lifetime (slow component) for $CsPbCl_3:Mn^{2+}$ (9, 20, and 32 atom %) NCs as a function of temperature. (a) Evolution of lifetime of $CsPbCl_3:Mn^{2+}$ (9, 20, and 32 atom %) NCs with temperature. (b) Three-level fitting of the long decay component of $CsPbCl_3:Mn^{2+}$ (20 atom %) NCs exciton decay versus temperature.

an energy difference of ∼19 meV for the dark−bright state splitting. This value is in good agreement with the ∼14 meV splitting for $CsPbCl_3$ NCs calculated from the influence of magnetic-field-induced mixing of dark and bright states, which influences the decay rate of the fast component of the exciton emission.[19]

The present results provide evidence for a normal splitting of the exciton state in $CsPbCl_3$ and can explain earlier observations that led to a model with an inverted dark−bright state splitting in $CsPbX_3$ NCs. To obtain conclusive evidence, it will be interesting to conduct temperature-dependent lifetime measurements on single $Mn^{2+}$-doped $CsPbCl_3$ NCs and search for the weak, temperature-dependent slow dark state emission in single Mn-doped NCs. Here, the origin of the anomalous exciton decay behavior is assigned to unusually slow phonon relaxation between excitonic states in $CsPbCl_3$ NCs. It will be interesting to verify this slow relaxation by other techniques, e.g., pump−probe experiments, and by theoretical calculations to better understand why phonon relaxation is hampered in halide perovskite NCs.

## CONCLUSIONS

In summary, we have investigated temperature dependence of exciton decay dynamics in Mn-doped $CsPbCl_3$ NCs. Upon cooling, the exciton decay time initially lengthens. A rise time is observed below 150 K, indicating slow phonon relaxation dynamics feeding the exciton state. At temperatures below 75 K, the decay becomes strongly biexponential with a fast decay component that is assigned to the bright state emission and a weak temperature-dependent slow component that is assigned to the dark state emission. The results are explained by a normal exciton energy level scheme with a higher-bright and lower-energy dark state combined with an extremely slow bright−dark state relaxation at cryogenic temperatures. In Mn-doped $CsPbCl_3$ NCs, the relaxation is an order of magnitude faster than that in undoped $CsPbCl_3$, which explains why the dark state emission, albeit weak, is more easily observed in Mn-doped $CsPbCl_3$ NCs.

## ASSOCIATED CONTENT

### Supporting Information

The Supporting Information is available free of charge on the ACS Publications website at DOI: 10.1021/acs.jpcc.8b12035.

Additional emission spectra and decay curves: Figure S1, normalized emission spectra of $CsPbCl_3:xMn^{2+}$ NCs; Figure S2, optical properties of $CsPbCl_3:xMn^{2+}$; and Figures S3−S9, exciton emission decay curve of pure $CsPbCl_3$, $CsPbCl_3:Mn^{2+}$ (1 atom %) NCs, $CsPbCl_3:Mn^{2+}$ (3 atom %), $CsPbCl_3:Mn^{2+}$ (41 atom %), $CsPbCl_3:Mn^{2+}$ (9 atom %) NCs; Figure S8, exciton emission decay curves of $CsPbCl_3:Mn^{2+}$ (20 atom %), and $CsPbCl_3:Mn^{2+}$ (32 atom %) NCs, respectively (PDF)

## AUTHOR INFORMATION

### Corresponding Author

*E-mail: A.Meijerink@uu.nl.

### ORCID

Andries Meijerink: 0000-0003-3573-9289

### Notes

The authors declare no competing financial interest.

## ACKNOWLEDGMENTS

This work is supported by the China Scholarship Council-Utrecht University Ph.D. Program (201404910557).

## REFERENCES

(1) Kovalenko, M. V.; Protesescu, L.; Bodnarchuk, M. I. Properties and Potential Optoelectronic Applications of Lead Halide Perovskite Nanocrystals. *Science* **2017**, *358*, 745−750.

(2) Stranks, S. D.; Snaith, H. J. Metal-halide Perovskites for Photovoltaic and Light-emitting Devices. *Nat. Nanotechnol.* **2015**, *10*, 391−402.

(3) Akkerman, Q. A.; Rainò, G.; Kovalenko, M. V.; Manna, L. Genesis, Challenges and Opportunities for Colloidal Lead Halide Perovskite Nanocrystals. *Nat. Mater.* **2018**, *17*, 394−405.

(4) Veldhuis, S. A.; Boix, P. P.; Yantara, N.; Li, M.; Sum, T. C.; Mathews, N.; Mhaisalkar, S. G. Perovskite Materials for Light-Emitting Diodes and Lasers. *Adv. Mater.* **2016**, *28*, 6804−6834.



DOI: 10.1021/acs.jpcc.8b12035
J. Phys. Chem. C 2019, 123, 979−984

(5) Protesescu, L.; Yakunin, S.; Bodnarchuk, M. I.; Krieg, F.; Caputo, R.; Hendon, C. H.; Yang, R.; Walsh, A.; Kovalenko, M. V. Nanocrystals of Cesium Lead Halide Perovskites ($CsPbX_3$, X = Cl, Br, and I): Novel Optoelectronic Materials Showing Bright Emission with Wide Color Gamut. *Nano Lett.* **2015**, *15*, 3692−3696.
(6) Liu, W.; Lin, Q.; Li, H.; Wu, K.; Robel, I.; Pietryga, J. M.; Klimov, V. I. $Mn^{2+}$-Doped Lead Halide Perovskite Nanocrystals with Dual-Color Emission Controlled by Halide Content. *J. Am. Chem. Soc.* **2016**, *138*, 14954−14961.
(7) Xu, K.; Lin, C. C.; Xie, X.; Meijerink, A. Efficient and Stable Luminescence from $Mn^{2+}$ in Core and Core−Isocrystalline Shell $CsPbCl_3$ Perovskite Nanocrystals. *Chem. Mater.* **2017**, *29*, 4265−4272.
(8) Milstein, T. J.; Kroupa, D. M.; Gamelin, D. R. Picosecond Quantum Cutting Generates Photoluminescence Quantum Yields Over 100% in Ytterbium-Doped $CsPbCl_3$ Nanocrystals. *Nano Lett.* **2018**, *18*, 3792−3799.
(9) Pan, G.; Bai, X.; Yang, D.; Chen, X.; Jing, P.; Qu, S.; Zhang, L.; Zhou, D.; Zhu, J.; Xu, W.; et al. Doping Lanthanide into Perovskite Nanocrystals: Highly Improved and Expanded Optical Properties. *Nano Lett.* **2017**, *17*, 8005−8011.
(10) Diroll, B. T.; Nedelcu, G.; Kovalenko, M. V.; Schaller, R. D. High-Temperature Photoluminescence of $CsPbX_3$ (X = Cl, Br, I) Nanocrystals. *Adv. Funct. Mater.* **2017**, *27*, 1606750−1606756.
(11) Chen, D.; Fang, G.; Chen, X. Silica-Coated Mn-Doped $CsPb(Cl/Br)_3$ Inorganic Perovskite Quantum Dots: Exciton-to-Mn Energy Transfer and Blue-Excitable Solid-State Lighting. *ACS Appl. Mater. Interfaces* **2017**, *9*, 40477−40487.
(12) Becker, M. A.; Vaxenburg, R.; Nedelcu, G.; Sercel, P. C.; Shabaev, A.; Mehl, M. J.; Michopoulos, J. G.; Lambrakos, S. G.; Bernstein, N.; Lyons, J. L.; et al. Bright Triplet Excitons in Caesium Lead Halide Perovskites. *Nature* **2018**, *553*, 189−193.
(13) Rainò, G.; Nedelcu, G.; Protesescu, L.; Bodnarchuk, M. I.; Kovalenko, M. V.; Mahrt, R. F.; Stöferle, T. Single Cesium Lead Halide Perovskite Nanocrystals at Low Temperature: Fast Single-Photon Emission, Reduced Blinking, and Exciton Fine Structure. *ACS Nano* **2016**, *10*, 2485−2490.
(14) Nirmal, M.; Norris, D. J.; Kuno, M.; Bawendi, M. G.; Efros, AlL.; Rosen, M. Observation of the "Dark Exciton" in CdSe Quantum Dots. *Phys. Rev. Lett.* **1995**, *75*, 3728−3731.
(15) de Mello Donegá, C.; Bode, M.; Meijerink, A. Size- and Temperature-dependence of Exciton Lifetimes in CdSe Quantum Dots. *Phys. Rev. B* **2006**, *74*, No. 085320.
(16) Efros, A.; Rosen, M. The Electronic Structure of Semiconductor Nanocrystals. *Annu. Rev. Mater. Sci.* **2000**, *30*, 475−521.
(17) Fu, M.; Tamarat, P.; Trebbia, J.; Bodnarchuk, M. I.; Kovalenko, M. V.; Even, J.; Lounis, B. Unraveling Exciton−Phonon Coupling in Individual $FAPbI_3$ Nanocrystals Emitting Near-Infrared Single Photons. *Nat. Commun.* **2018**, *9*, No. 3318.
(18) Canneson, D.; Shornikova, E. V.; Yakovlev, D. R.; Rogge, T.; Mitioglu, A. A.; Ballottin, M. V.; Christianen, P. C. M.; Lhuillier, E.; Bayer, M.; Biadala, L. Negatively Charged and Dark Excitons in $CsPbBr_3$ Perovskite Nanocrystals Revealed by High Magnetic Fields. *Nano Lett.* **2017**, *17*, 6177−6183.
(19) Chen, L.; Li, B.; Zhang, C.; Huang, X.; Wang, X.; Xiao, M. Composition-Dependent Energy Splitting between Bright and Dark Excitons in Lead Halide Perovskite Nanocrystals. *Nano Lett.* **2018**, *18*, 2074−2080.
(20) Yuan, X.; Ji, S.; De Siena, M. C.; Fei, L.; Zhao, Z.; Wang, Y.; Li, H.; Zhao, J.; Gamelin, D. R. Photoluminescence Temperature Dependence, Dynamics, and Quantum Efficiencies in $Mn^{2+}$-Doped $CsPbCl_3$ Perovskite Nanocrystals with Varied Dopant Concentration. *Chem. Mater.* **2017**, *29*, 8003−8011.
(21) Xu, K.; Meijerink, A. Tuning Exciton−$Mn^{2+}$ Energy Transfer in Mixed Halide Perovskite Nanocrystals. *Chem. Mater.* **2018**, *30*, 5346−5352.
(22) Granados del Águila, A.; Pettinari, G.; Groeneveld, E.; de Mello Donegá, C.; Vanmaekelbergh, D.; Maan, J. C.; Christianen, P. C. M. Optical Spectroscopy of Dark and Bright Excitons in CdSe Nanocrystals in High Magnetic Fields. *J. Phys. Chem. C* **2017**, *121*, 23693−23704.


DOI: 10.1021/acs.jpcc.8b12035
*J. Phys. Chem. C* 2019, 123, 979−984